Alpinia katsumadai Hayata induces growth inhibition and autophagy-related apoptosis by regulating the AMPK and Akt/mTOR/p70S6K signaling pathways in cancer cells

WEIXIAO AN[1,2*], YUXI ZHANG[1*], HONGLIN LAI[3], YANGYANG ZHANG[4], HONGMEI ZHANG[5], GE ZHAO[6], MINGHUA LIU[1], YANG LI[7], XIUKUN LIN[8] and SHOUSONG CAO[1]

[1]Department of Pharmacology, School of Pharmacy, Southwest Medical University, Luzhou, Sichuan 646000; [2]Department of Pharmacy, Chengdu Second People's Hospital, Chengdu, Sichuan 610021; [3]Department of Pharmacy, Affiliated Hospital of Traditional Chinese Medicine, Southwest Medical University, Luzhou, Sichuan 646000; [4]Department of Pharmacy, Dongying Hospital of Traditional Chinese Medicine, Dongying, Shandong 257055; [5]Rizhao Hospital of Traditional Chinese Medicine, Rizhao, Shandong 276801; [6]Department of Pharmacology, School of Pharmacy, Chengdu University of Traditional Chinese Medicine, Chengdu, Sichuan 611137; [7]Department of International Trade, School of International Traded and Economics, University of International Business and Economics, Beijing 100029; [8]Delisi Group Co. Ltd., Zhucheng, Shandong 262200, P.R. China

Received March 3, 2022; Accepted May 17, 2022

DOI: 10.3892/or.2022.8353

Abstract. *Alpinia katsumadai Hayata* (AKH), a widely used traditional Chinese medicine, exerts various biological functions, including anti-inflammatory, antioxidant, anti-microbial and anti-asthmatic effects. However, studies on its anticancer activity and associated mechanisms are limited. The present study investigated the effects of ethanol extract from AKH on the viability of various human cancer and normal liver LX-2 cells using Cell Counting Kit-8 assay. Apoptosis was detected by Hoechst 33342/PI staining and Annexin-V-FITC/PI double staining. Autophagy was examined by Ad-GFP-LC3B transfection. The association between AKH-induced autophagy and apoptosis was investigated by pre-treatment of the cells with the autophagy inhibitors, 3-methyladenine (3MA) and bafilomycin A1 (Baf-A1), followed by treatment with AKH. The expression levels of cleaved poly(ADP-ribose) polymerase (PARP), caspase-8, caspase-3, caspase-9, phosphorylated (p-) AMP-activated protein kinase (AMPK), Akt, mTOR and p70S6K were examined using western blot analysis. The *in vivo* antitumor activity of AKH was investigated in nude mice bearing A549 lung cancer xenografts. The components of AKH were detected by liquid chromatography mass spectrometry-ion trap-time-of-flight mass spectrometry. The results revealed that AKH significantly inhibited the proliferation of various cancer cells with the half maximal inhibitory concentration (IC_{50}) values of 203-284 μg/ml; however, its inhibitory effect was much less prominent against normal liver LX-2 cells with an IC_{50} value of 395 μg/ml. AKH markedly induced apoptosis and autophagy, and upregulated the protein expression of cleaved-caspase-3, caspase-8, caspase-9 and cleaved PARP in a concentration-dependent manner. Of note, the autophagy inhibitors (3MA and Baf-A1) significantly attenuated its pro-apoptotic effects on human pancreatic cancer Panc-28 and lung cancer A549 cells. Furthermore, AKH significantly increased the levels of p-AMPK, and decreased those of p-Akt, p-mTOR and p-p70S6K in Panc-28 and A549 cells. AKH markedly inhibited the growth of A549 tumor xenografts *in vivo*. In addition, a total of nine compounds were detected from AKH. The present study demonstrates that AKH markedly inhibits the growth and induces autophagy-related apoptosis in cancer cells by regulating the AMPK and Akt/mTOR/p70S6K signaling pathways. AKH and/or its active fractions may thus have potential to be developed as novel anticancer agents for clinical use.

Correspondence to: Dr Shousong Cao, Department of Pharmacology, School of Pharmacy, Southwest Medical University, 319 Zhongshan Road, Jiangyang, Luzhou, Sichuan 646000, P.R. China
E-mail: shousongc@gmail.com

Dr Xiukun Lin, Delisi Group Co. Ltd., 1 Lutai Avenue, Zhucheng, Shandong 262200, P.R. China
E-mail: xiukunlin@126.com

*Contributed equally

Key words: *Alpinia katsumadai Hayata*, apoptosis, autophagy, adenosine 5'-monophosphate-activated protein kinase, serine-threonine kinase/mammalian target of rapamycin/70-kDa ribosomal protein S6 kinase signaling pathway

Introduction

Cancer is one of the major issues affecting public health and is considered the leading cause of mortality worldwide (1,2). There

were 1,806,590 new cancer cases and 606,520 cancer-related deaths in the United States in 2020 (2). The major treatment strategies for cancer include surgery, radiotherapy, chemotherapy, biotherapy and immunotherapy. Moreover, traditional Chinese medicine (TCM) has gradually become a hot topic of cancer research and therapy in recent years due to its therapeutic efficacy (particularly in combination with Western medicine), mild side-effects, its cost-effectiveness and widely available sources. However, its scope of clinical application in cancer therapy is limited by complex components and unclear therapeutic targets (3,4). Therefore, the use of modern science and technology to examine the effects of active components from TCM and the associated molecular mechanisms in cancer cells and animal models of human cancer is a crucial and feasible strategy for the discovery and development of novel anticancer drugs and cancer therapeutics.

Apoptosis is a type of programmed cell death accompanied by cell membrane contraction, nucleus fragmentation, chromatin condensation and chromosome DNA breakage (5). The study of apoptosis has been an emerging field in cancer research for several years (5). Apoptosis can be initiated either through the extrinsic (death receptor-mediated) or the intrinsic (mitochondria-mediated) pathway, which activates the initiator caspases for the further activation of the caspase cascade and caspase-3 to induce cellular apoptosis (6,7). Autophagy is a highly self-regulated catabolic process in eukaryotic organisms, and similar to apoptosis, it plays a critical role in the growth and development of organisms (8,9). Autophagy can potentially function as the dual nature mechanisms of pro-survival and pro-death in the initiation and progression of cancer (10). The pro-survival effects of autophagy on cancer are mainly due to a mechanism that permits increased tolerance to stress, obtaining ATP and metabolic intermediates (11). However, an increase in the autophagic flux may induce cell death as a tumor-suppressive mechanism (12). There are two well-known signaling pathways involved in the autophagy progress, namely the PI3K/Akt/mTOR/p70S6K and Ras/Raf/MEK1/2/ERK1/2 signaling pathways (13,14). It has been reported that autophagy can be negatively controlled by mTOR, while AMP-activated protein kinase (AMPK) can inhibit mTOR to govern autophagy (15). Furthermore, a connection between autophagy and apoptosis exists; on the one hand, autophagy occurs before apoptosis and persistent autophagy can induce cell death and increase apoptosis; on the other hand, autophagy serves as a protector to prevent cells from undergoing apoptosis by inhibiting the release of apoptotic factors (16,17).

TCM has long been widely used for the prevention and treatment of various diseases, including cancer in China and other Asian countries. TCM has attracted increasing attention and has become an emerging field for anticancer drug discoveries and development due to its wide availability in nature and the fact that it can be easily obtained; moreover, some active components isolated and extracted from TCM have exhibited significant antitumor activity with less side-effects compared to commonly used chemotherapeutic agents in cancer therapy (3,18,19).

Alpinia katsumadai Hayata (AKH) has long been widely used as a TCM in China and Korea. AKH was recorded in Chinese Pharmacopoeia as being pungent in flavor, 'warm' in nature, and attributive to the stomach and spleen meridians (20). AKH is believed to promote qi, disperse cold, relieve pain, dry dampness and stop vomiting (20). AKH is commonly used to treat internal obstruction, abdominal distension, belching and retching counterflow, as well as to increase appetite (20). Modern pharmacological studies have demonstrated that AKH has anti-bacterial, antioxidant, anti-inflammatory and anti-asthmatic activities (6,21). Previous studies have also proven that the active components of AKH can induce the apoptosis and autophagy of cancer cells (22,23). However, studies on the effects of AKH on the proliferation, apoptosis and autophagy of cancer cells, as well as on the associated mechanisms are limited.

The present study investigated the *in vitro* effects of an ethanol (EtOH) extract of AKH on cell proliferation using a Cell Counting Kit-8 (CCK-8) assay, apoptosis using Hoechst 33342/propidium iodide (PI) staining and Annexin-V-fluorescein isothiocyanate (FITC)/PI double staining and autophagy using Ad-GFP-LC3B transfection in cancer cells, respectively. In addition, the association between AKH-induced apoptosis and autophagy was examined using the autophagy inhibitors, 3-methyladenine (3MA, M9281) and Baflomycin A1 (Baf-A1). The expression levels of cleavage poly(ADP-ribose) polymerase (PARP), caspase-8, caspase-3 and caspase-9 were examined by western blot analysis. Furthermore, the *in vivo* antitumor effects of AKH were evaluated in the nude mice with A549 lung tumor xenografts. The components of AKH were detected by liquid chromatography mass spectrometry (LCMS)-ion trap (IT)-time-of-flight (TOF) mass spectrometry.

Materials and methods

Preparation of AKH. The seeds of AKH (cat. no. T000500063) were purchased from Sichuan Hongpu Pharmaceutical Co., Ltd. A total of 10 kg dehydrated powdered seeds of AKH were extracted with 95% EtOH (Chengdu Chron Chemicals Co., Ltd.) for 48 h at room temperature. The EtOH extraction was concentrated with a rotary evaporator under 50˚C under reduced pressure as previously described (24).

Chemicals and reagents. 3MA was purchased from MilliporeSigma. RPMI-1640 medium, fetal bovine serum (FBS) and dimethyl sulfoxide (DMSO) were purchased from Gibco; Thermo Fisher Scientific, Inc. The Hoechst 33342/PI kit and Baf-A1 were purchased from Beijing Solarbio Science & Technology Co., Ltd. The Cell Counting Kit (CCK)-8 kit, Ad-GFP-LC3B and actin mouse monoclonal antibody (cat. no. AF0003) were purchased from the Beyotime Institute of Biotechnology. The Annexin V-FITC apoptosis detection kit was purchased from BD Biosciences. The pro-caspase-3 (cat. no. ab32150), cleaved caspase-3 (cat. no. ab32042), caspase-8 (cat. no. ab32397), caspase-9 (cat. no. ab32068), PARP (cat. no, ab32138) and cleaved PARP (cat. no. ab32561) antibodies were purchased from Abcam. LC3B (cat. no. 2775S), Beclin-1 (cat. no. 3738S), AMPK (cat. no. 2532S), phosphorylated (p-)AMPK at Ser 485 (cat. no. 4184S), Akt (cat. no. 9272S), p-Akt at Ser473 (cat. no. 9271S), mTOR (cat. no. 2972S), p-mTOR at Ser2448 (cat. no. 2971S), p70S6K (cat. no. 9202S) and p-p70S6K at

Thr389 (cat. no. 9205S) antibodies were purchased from Cell Signaling Technology, Inc.

Cells and cell culture. The human lung cancer A549 (cat. no. CCL-185), breast cancer MDA-MB-468 (cat. no. HTB-132), cervical cancer HeLa (cat. no. CCL-2), glioblastoma of unknown origin U87 (cat. no. HTB-14) and colon cancer HCT-116 (cat. no. CCL-247) cell lines were purchased from the American Type Culture Collection (ATCC). The human melanoma A875 (cat. no. CL-0255) and normal hepatic stellate LX-2 (cat. no. CL-0560) cell lines were purchased from Procell Life Science & Technology. The human pancreatic cancer Panc-28 cell line was kindly provided by Dr Joshua Liao (University of Minnesota, Austin, MN, USA). All cancer cells were cultured in RPMI-1640 medium, whereas the LX-2 cells were cultured in Dulbecco's modified Eagle's medium (DMEM) supplemented with 10% FBS and 1% penicillin/streptomycin and maintained in an atmosphere of 5% carbon dioxide (CO_2) at 37˚C and renewed with new medium every 3-5 days. The LX-2 cells were analyzed by short tandem repeat profiling, cell morphology and karyotyping assay. All cell lines were verified on the Cellosaurus database and it was confirmed that they were not considered problematic for use.

Cell viability assay. The effect of AKH on the viability of various cancer cells and normal hepatic stellate LX-2 cells was evaluated by CCK-8 assay. Briefly, cells (>90% confluency, $5x10^3$ cells/well) were seeded in 96-well culture plates. Following overnight incubation, the cells were treated with the solvent solution (vehicle control) or various concentrations of AKH (50, 100, 150, 200, 300 and 400 μg/ml) for 48 h, respectively. For the study of time-dependent effects of AKH on cell growth inhibition, the Panc-28 and A549 cells (the two most sensitive cells to AKH treatment (Table I and Fig. 1A) were seeded ($5x10^3$ cells/well) and treated with the vehicle control or AKH at 100, 150, 200, 250, 300 and 400 μg/ml for 24, 48 and 72 h, respectively. Subsequently, 10% CCK-8 solution (10 μl/well) were added to each well and the cells were incubated for an additional 1 h at 37˚C. The products of CCK-8 formazan were estimated by measuring the optical density (OD) at a 450 nm absorbance using a microplate reader (Model 680, Bio-Rad Laboratories, Inc.). Cell viability was calculated as the OD of the drug-treated sample/OD of the control sample x100%. The values of half inhibitory concentration (IC_{50}) were calculated by regression analysis using SPSS 20.0 statistical software (IBM Corporation). All experiments were performed for at least three times in triplicate.

Hoechst 33342/PI double staining assay. Apoptotic cancer cells were initially detected using the Hoechst 33342/PI double stain apoptosis detection kit (Beijing Solarbio Science & Technology Co., Ltd.) following the manufacturer's instructions. Briefly, the Panc-28 or A549 cells (>90% confluency) were seeded in six-well plates at a density of $3x10^5$ cells/well. The cells were treated with the vehicle control or AKH at 150, 200 and 250 μg/ml for 48 h following 24 h of culture. The medium was then removed, and the cells were washed with PBS for three times in 15 min (5 min each). Finally, the cells were stained with Hoechst 33342/PI kit in the dark for 30 min at room temperature and apoptotic cells were observed under a Leica DM6 B fluorescence microscope (Leica Microsystems

Table I. IC_{50} values of AKH in various cell lines determined by CCK-8 assay.

Cell line	Cell type	IC_{50} (μg/ml)
Panc-28	Human pancreatic cancer	202.7±6.4
A549	Human lung cancer	219.0±9.9
MDA-MB-468	Human breast cancer	234.7±8.4
Hela	Human cervical cancer	236.2±8.8
A875	Human melanoma cancer	259.6±11.3
U87	Human glioblastoma of unknown origin	262.0±15.9
HCT-116	Human colon cancer	284.0±9.1
LX-2	Human hepatic stellate cell	395.4±2.21

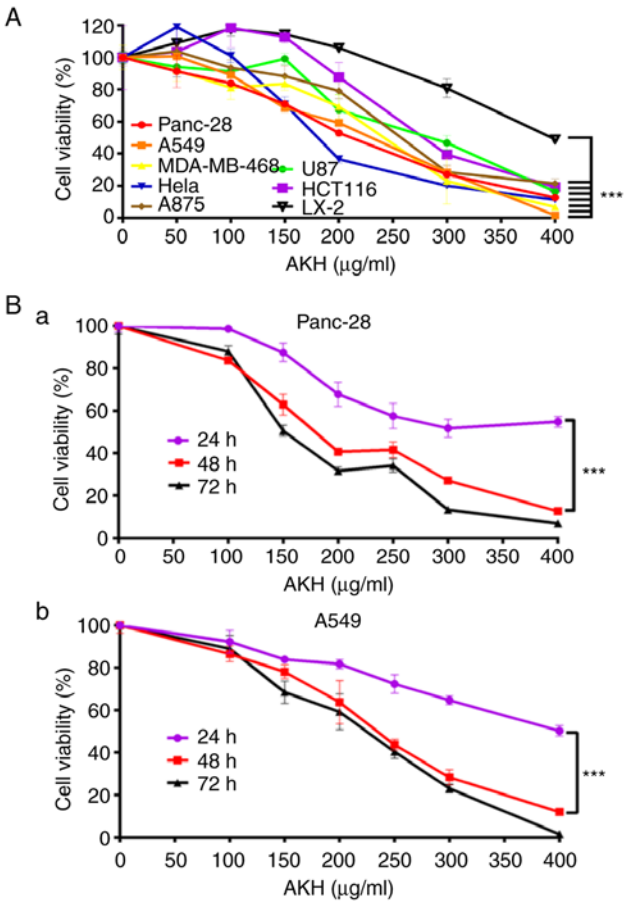

Figure 1. AKH inhibits the proliferation of various cancer cells, as demonstrated using CCK-8 assay. (A) Viability of Panc-28, A549, MDA-MB-468, Hela, A875, U87, HCT-116 and LX-2 cells following treatment with the vehicle control or various concentrations of AKH (50, 100, 150, 200, 300 and 400 μg/ml) for 48 h. (B) Time-effects of AKH on (a) Panc-28 and (b) A549 cells. The cells were treated with the vehicle control or AKH at 100, 150, 200, 250, 300 and 400 μg/ml for 24, 48, or 72 h, respectively. The data are representative of three independent experiments (n=3) run in triplicate and are expressed as the mean ± SD. ***P<0.001 vs. LX-2 cells in A and vs. 24 h in B (determined using one-way ANOVA). AKH, *Alpinia katsumadai Hayata*.

GmbH). All experiments were performed for at least three times in triplicate.

Annexin V/PI staining assay. The detection of the apoptosis of Panc-28 and A549 cells was also performed using flow cytometric analysis with the Annexin V-FITC apoptosis detection kit according to the manufacturer's protocol as described in a previous study by the authors (25). Briefly, ~5x10^5 cells (>90% confluency) were seeded in each well of six-well culture plates and cultured overnight at 37˚C in an incubator. Various concentrations (150, 200 and 250 μg/ml) of AKH were added to the plates and incubated at 37˚C for 48 h. The cells were harvested by trypsinization, washed with PBS twice, and resuspended in 1X binding buffer at a concentration of 1x10^6 cells. Subsequently, 100 μl (1x10^6) cells were mixed with 5 μl of Annexin V-FITC and 5 μl PI and incubated at room temperature in the dark for 15 min. The samples (500 μl) were analyzed for apoptotic cells using a flow cytometer (Becton, Dickinson and Company). All experiments were performed for at least three times in triplicate.

Ad-GFP-LC3B transfection. To detect the formation of autophagosomes, the Panc-28 and A549 cells were transfected with Ad-GFP-LC3B (Beyotime Institute of Biotechnology) following the manufacturer's instructions. Briefly, the cells (>90% confluency) were seeded in a 24-well plate at a density of 5x10^4 cells/well and transfected with Ad-GFP-LC3B at a multiplicity of 40 with 2x10^6 plaque forming units (pfu) adenovirus for 24 h at room temperature. The cells were then treated with medium (control) or AKH (250 μg/ml) for 24 h, respectively. They were then fixed with 4% polyoxymethylene and observed under a Leica DM6 B fluorescence microscope at x40 magnification (Leica Microsystems GmbH). All experiments were performed for at least three times in triplicate.

Western blot analysis. The Panc-28 and A549 cells (>90% confluency) were seeded in six-well plates at a density of 5x10^5 cells/well. Following 24 h of incubation, the cells were treated with the solvent solution or AKH at 150, 200 and 250 μg/ml for 48 h. The cells were then collected by centrifugation at 1,500 x g at room temperature for 5 min and lysed in ice-cold RIPA lysate buffer as described in a previous study by the authors (25). The protein concentrations were determined using the BCA method. Subsequently, equal amounts of proteins (30-40 μg) were separated by 10% sodium dodecyl sulphate (SDS)-polyacrylamide gel electrophoresis (PAGE) and transferred onto polyvinylidene fluoride (PVDF) membranes (EMD Millipore). Non-specific binds were blocked with 5% non-fat dry milk in 1X TBST buffer (1X TBS and 0.1% Tween-20) for 1 h at room temperature and subsequently incubated with the corresponding primary antibodies (1:1,000) of caspase-8, caspase-3, caspase-9, PARP, LC3B, Beclin-1, Akt, p-Akt, mTOR, p-mTOR, AMPK, p-AMPK, p70S6K, p-p70S6K or actin overnight at 4˚C. The membranes were washed four times (10 min each) with 1X TBST buffer and incubated with horseradish peroxidase (HRP)-conjugated goat anti-mouse (cat. no. A0216) or anti-rabbit secondary antibodies (cat. no. A0208, Beyotime Institute of Biotechnology) at 1:1,000 for 1 h at room temperature on a shaker and washed four times with 1X TBST buffer for 40 min. Actin was used as a loading control. Finally, the membranes were developed and visualized using the ECL Western Blotting detection kit (cat. no. 32109, Thermo Fisher Scientific Inc.) after washing with 1X TBST four times. The OD values of the blots were measured using ImageJ software version 1.52a (National Institutes of Health). All samples were performed for three times in triplicate.

Antitumor activity of AKH against A549 tumor xenografts in nude mice in vivo. Female athymic Balb/C nude mice (6-8 weeks old; body weight, 18-20 g) were purchased from Chengdu Dasuo Laboratory animal Co., Ltd. and housed in a specific pathogen-free (SPF) facility with a constant laboratory condition of a 12-h light/dark cycle and provided with food and water *ad libitum*. A549 tumor xenografts were initially established in nude mice by a subcutaneous (s.c.) injection of cultured A549 cells (1x10^7 cells/ml in the logarithmical stage with >90% confluency) in 150 μl of serum-free RPMI-1640 medium into the right flanks of the mice. The tumor xenografts were subsequently passed several generations by transplantation of ~50 mg non-necrotic tumor tissues into the right flanks of mice with the help of a trocar prior to treatment, which was initiated 2 weeks later when the tumors reached ~100 mm^3 (mg) as previously described (26,27). The mice were randomly divided into four groups with 5 mice in each group and treated as follows: i) Normal saline (negative vehicle control); ii) cisplatin (Jiangsu Hansoh Pharmaceutical Co., Ltd.) 5 mg/kg (positive control); iii) AKH at 100 mg/kg; and iv) AKH at 400 mg/kg. The powder of AKH EtOH extract was first dissolved in normal saline and the solution was administered to the mice so there was no converted into an EtOH extract in the body. AKH and normal saline were orally administered by gavage once a day for 12 consecutive days and cisplatin by intraperitoneal (i.p.) injection every 3 days (on days 0, 3, 6, 9 and 12, for a total of five doses) with an ~0.2 ml volume per 20 g mouse weight (28). The body weights of the mice and tumor volumes were monitored every 3 days during treatment. The tumors were measured by the longest axis (L) and shortest axis (W) with the help of a Vernier caliper and the tumor volume (mm^3) or weight (mg) was calculated using the following formula: 1/2 (L x W^2) (mm^3) (26,28). At the end of the experiment (24 h after the final treatment) for a duration of 4 weeks, all mice were euthanized by rapid cervical dislocation, and the tumors were removed and weighed to obtain images and calculate the rate of tumor inhibition. The specific criteria used to determine euthanasia timepoints for the mice was when the tumor reached ~2,000 mg (mm^3) or 20% of body weight loss. Death was verified by monitoring breathing, heartbeat, flexor reflex and corneal contact response. The tumor growth inhibition (TGI) was calculated by the mean tumor volume (weight) of the treatment group (TG)/relative to the control group (CG) using the following formula: (MTWTG-MTWCG) ÷ MTWCG x100% (26,27).

All animal experiments were approved (permit no. 201802-112) by the Institutional Animal Care and Use Committee of Southwest Medical University (Luzhou, China) and strictly followed the guidelines for the investigation of experimental pain in conscious

animals for improving animal welfare to minimize animal suffering (29).

Analysis of the composition of AKH by LCMS-IT-TOF assay. LC-MS analysis of the composition of AKH was performed using a Shimadzu LCMS-IT-TOF mass spectrometer (Shimadzu Corp.). The samples of AKH were separated on an Agilent Eclipse plus C18 column (100x2.1 mm i.d. 1.8 μM particle size; Agilent Technologies, Inc.). The separation process was followed the gradient elution procedure. Chromatographic analysis was used the mobile phase A, which was composed of acetonitrile modified with 0.5% formic acid, while the mobile phase B was composed of water modified with 0.5% formic acid. The linear gradient was as A:B=40-90% for 24 min. The flow rate was 0.2 ml/min and the column temperature was 30˚C. The injection volume was 5 μl. For mass detection, the following parameters were used for analytical MS: Nozzle voltage, 4.5 KV (+)/-3.5 KV (-) in the detection modes of positive ion and negative ion; electrospray ionization (ESI) voltage, 1.65 KV; nebulizing gas (N2) flow rate, 1.5 l/min; and drying gas flow rate, 10.0 l/min. The desolation line was heated to 250˚C and the heat block was heated to 450˚C. Collision-induced dissociation gas pressure was set to 230 kPa. The MS data were acquired from m/z 100 to 2,000. The data were analyzed using Lab Solutions software (version 5.75, Shimadzu Corp.).

Statistical analysis. Data were analyzed using SPSS 20.0 statistical software (IBM Corporation) and presented as the mean ± standard deviation (SD). One-way analysis of variance (ANOVA) and the univariate analysis of general linear model were used to determine statistical significance. Tukey's test was applied as the post hoc test. The data of western blot analysis were quantified using Image J software version 1.52a (National Institute of Health). A value of $P<0.05$ was considered to indicate a statistically significant difference.

Results

AKH inhibits the proliferation of various cancer cells. The present study first investigated the inhibitory effects of AKH at multiple concentrations (0, 50, 100, 150, 200, 300 and 400 μg/ml) on the proliferation of various cancer cells and compared to normal hepatic stellate LX-2 cells by CCK-8 assay. The results revealed that AKH significantly ($P<0.001$) inhibited the growth of various cancer cells in a concentration-dependent manner; however, it exerted a weak inhibitory effect on the LX-2 cells (Fig. 1A). The IC_{50} values of AKH were 202.7±6.4, 219.7±9.9, 234.7±8.4, 236.2±8.8, 259.6±11.3, 262.0±15.9, 284.0±9.1 and 395.4±2, 21 μg/ml for the Panc-28, A549, MDA-MB-468, HeLa, A875, U87, HCT-116 and LX-2 cells, respectively (Table I). These results indicated that AKH exerted the most potent cytotoxic effect on the Panc-28 and A549cells. Subsequently, the time-dependent effects of AKH on the growth inhibition in Panc-28 and A549 cells were examined by treating the cells with AKH at 0 (control), 100, 150, 200, 250, 300 and 400 μg/ml for 24, 48 and 72 h, respectively. The results revealed that the inhibitory effects of AKH on the Panc-28 and A549 cells were time-dependent; AKH was more effective at 48 and 72 h than at 24 h ($P<0.001$); no statistically significant difference was observed between the 48 and 72 h time points ($P>0.05$), although the inhibitory effect of AKH was the most prominent at 72 h (Fig. 1Ba and Bb).

AKH induces the apoptosis of Panc-28 and A549 cells. Apoptosis is closely related to the fate of cancer and is one of the key targets for novel anticancer drug discovery and development (19). Therefore, the present study examined the effects of AKH on the apoptosis of Panc-28 and A549 cells using Hoechst 33342/PI staining assay. The results demonstrated that treatment with AKH at 150, 200 and 250 μg/ml for 48 h significantly induced cellular apoptosis in a concentration-dependent manner; the cells displayed typical morphological features of apoptosis, including chromatin condensation, nuclear shrinkage, and the formation of apoptotic bodies (Fig. 2A and B).

For the quantitative analysis of the effects of AKH on apoptosis induction, flow cytometric analysis was then performed using Annexin-V-FITC/PI double staining assay in the Panc-28 and A549 cells. The data demonstrated that treatment with AKH for 48 h markedly induced apoptosis in a concentration-dependent manner; the apoptotic rates were 7.23±0.45 and 7.58±0.93%, 9.68±0.73 and 12.68±0.53%, 16.89±1.22 and 16.23±0.52%, and 36.45±1.65 and 32.35±.26% for the Panc-28 and A549 cells treated with the vehicle (control), or 150, 200 and 250 μg/ml of AKH, respectively (Fig. 2C-F).

To further investigate the underlying mechanisms of the AKH-induced apoptosis of the cancer cells, the expression of cleaved PARP, caspase-8, caspase-3 and caspase-9 was examined using western blot analysis of the Panc-28 and A549 cells. The results revealed that the relative expression levels of the apoptotic proteins, cleaved PARP, caspase-8, cleaved caspase-3 and caspase-9, were significantly increased in a concentration-dependent manner following treatment with AKH (Fig. 2G and H). These data indicate that AKH markedly induced apoptosis and that apoptosis plays a crucial role in the inhibitory effects of AKH on the proliferation of cancer cells.

AKH induces autophagy and autophagy plays a role in the regulation of the apoptosis of Panc-28 and A549 cells. Autophagy plays a dual role in cancer initiation and progression, autophagy and apoptosis are highly interconnected in determining the fate of cancer cells (30,31). Therefore, the present study evaluated the effects of AKH on autophagy induction and the role of AKH-induced autophagy in the regulation of apoptosis. To examine the effects of AKH on autophagy, Panc-28 and A549 cells were transfected with Ad-GFP-LC3B and treated with the vehicle solution (control) and AKH (250 μg/ml) for 24 h. The results revealed that there were diffuse green spots in the control cells and evident green autophagy spots in the AKH-treated cells (Fig. 3A), indicating that AKH induced autophagy. The present study then further detected LC3-II formation after the transfected cells were treated with various concentrations of AKH (150, 200 and 250 μg/ml) for 48 h. The results revealed that the conversion of LC3-II and the expression of Beclin-1 were markedly

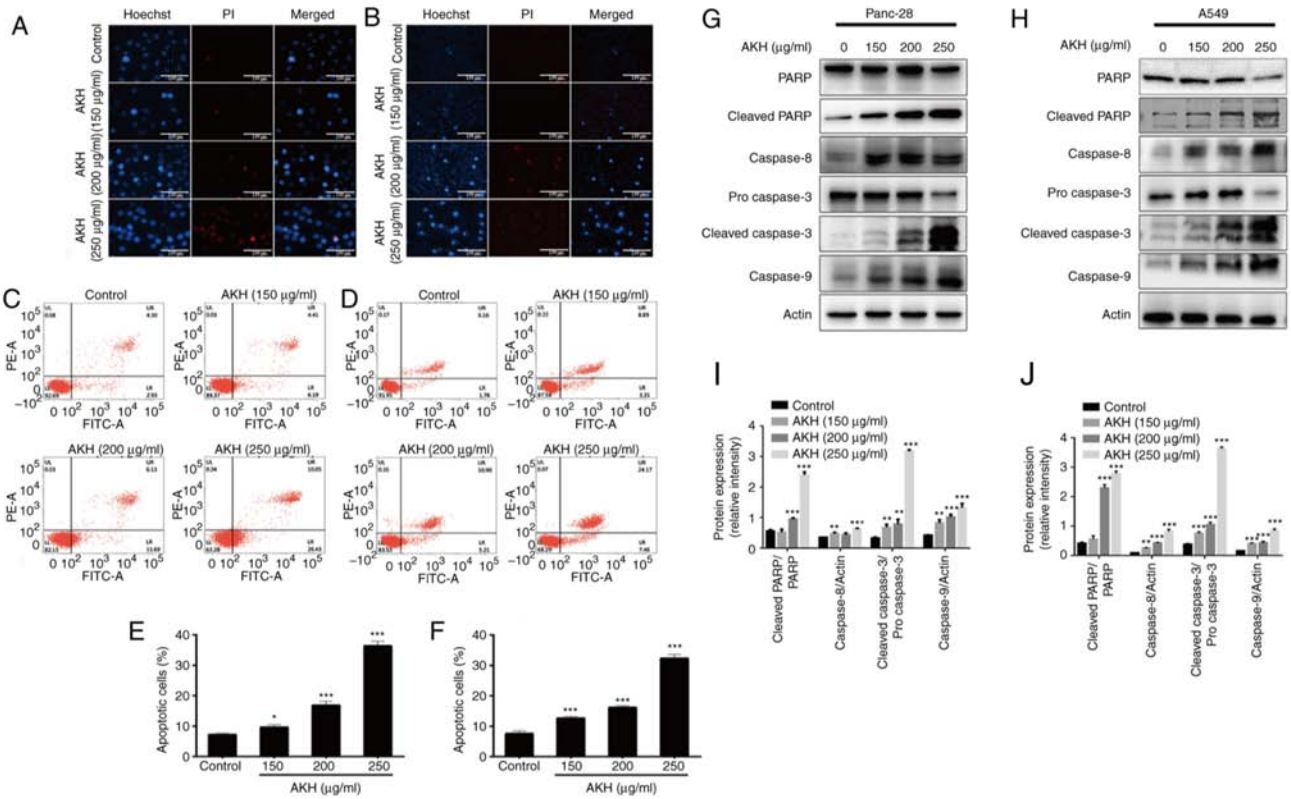

Figure 2. Effects of AKH on apoptosis and the expression of apoptosis-related proteins in Panc-28 and A549 cells. (A) The morphological features of apoptosis induced by AKH in Panc-28 by Hoechst 33342/PI staining assay. (B) The morphological features of apoptosis induced by AKH in A549 cells by Hoechst 33342/PI staining assay. (C) Analysis of apoptosis of Panc-28 cells examined by flow cytometry with Annexin-V-FITC/PI double staining assay. (D) Analysis of apoptosis of A549 cells by flow cytometry with Annexin-V-FITC/PI double staining assay. (E) Percentage of apoptotic Panc-28 cells. (F) Percentage of apoptotic A549 cells. (G) The expression of apoptosis-related proteins PARP, cleaved-PARP, caspase-8, pro-caspase-3, cleaved-caspase-3 and caspase-9 in Panc-28 cells by western blot analysis. (H) The expression of apoptosis-related proteins PARP, cleaved-PARP, caspase-8, pro-caspase-3, cleaved-caspase-3 and caspase-9 in A549 cells by western blot analysis. (I) The protein expression of cleaved-PARP/PARP, caspase-8, cleaved-caspase-3/pro-caspase 3 and caspase-9 in Panc-28 cells. (J) The protein expression of cleaved-PARP/PARP, caspase-8, cleaved-caspase-3/pro-caspase-3 and caspase-9 in A549 cells. Actin was used as a loading control. The cells were treated with the vehicle control or AKH at 150, 200 and 250 μg/ml for 48 h. The data are representative of three independent experiments (n=3) run in triplicate and are expressed as the mean ± SD. *P<0.05, **P<0.01 and ***P<0.001 vs. vehicle control (determined using one-way ANOVA). AKH, *Alpinia katsumadai Hayata;* PARP, poly(ADP-ribose)polymerase.

enhanced in a concentration-dependent manner in the Panc-28 and A549 cells (Fig. 3B-E).

To further investigate the association between AKH-induced autophagy and apoptosis, the Panc-28 and A549 cells were pre-treated with the autophagy inhibitors, 3MA (5 mM) or Baf-A1 (10 nM), for 24 h followed by treatment with AKH (250 μg/ml) for 48 h. The cells were then examined by flow cytometry and western blot analysis. The results of CCK-8 assay revealed that both the autophagy inhibitors, 3MA and Baf-A1, significantly decreased the inhibitory effects of AKH on the viability of the Panc-28 (P<0.001; Fig. 4A) and A549 (P<0.05 or P<0.01; Fig. 4B) cells. The flow cytometry data revealed that both 3MA and Baf-A1 significantly inhibited the apoptosis induced by AKH in the Panc-28 (P<0.01 or P<0.001; Fig. 4C) and A549 (P<0.05; Fig. 4D) cells. Moreover, the data of western blot analysis also demonstrated that 3MA and Baf-A1 markedly reduced the expression level of apoptosis- and autophagy-related proteins, such as cleaved PARP, pro- and cleaved caspase-3 and Beclin-1 in the Panc-28 and A549 cells (Fig. 4E and F). However, 3MA decreased the expression of LC3 due to inhibiting autophagosome formation; however, Baf-A1 increased the expression of LC3 by preventing lysosome degradation (Fig. 4E and F).

Effects of AKH on AMPK and Akt/mTOR/p70S6K in Panc-28 and A549 cells. AMPK and Akt/mTOR/p70S6K play a critical role in regulating both the apoptosis and autophagy of cancer cells (31-34). Therefore, the present study investigated the effects of AKH on the expression of proteins related to the AMPK and Akt/mTOR/p70S6K signaling pathways in Panc-28 and A549 cells by western blot analysis. The data demonstrated that AKH significantly increased the levels of p-AMPK and decreased those of p-Akt (P<0.01 or P<0.001) and subsequently decreased the levels of downstream target proteins of Akt, such as p-mTOR and p-70S6K (P<0.01 or P<0.001) in a concentration-dependent manner in both the Panc-28 and A549 cells (Fig. 5).

These data indicated that AKH significantly increased the levels of p-AMPK and decreased those of p-Akt, and its downstream target proteins, such as p-mTOR and p-70S6K in the Panc-28 and A549 cells.

AKH inhibits the growth of A549 tumor xenografts in nude mice in vivo. After completing the experiments to determine the effects of AKH on the growth inhibition and apoptosis/autophagy induction of the Panc-28 and A549 cells *in vitro*, the present study further evaluated the *in vivo*

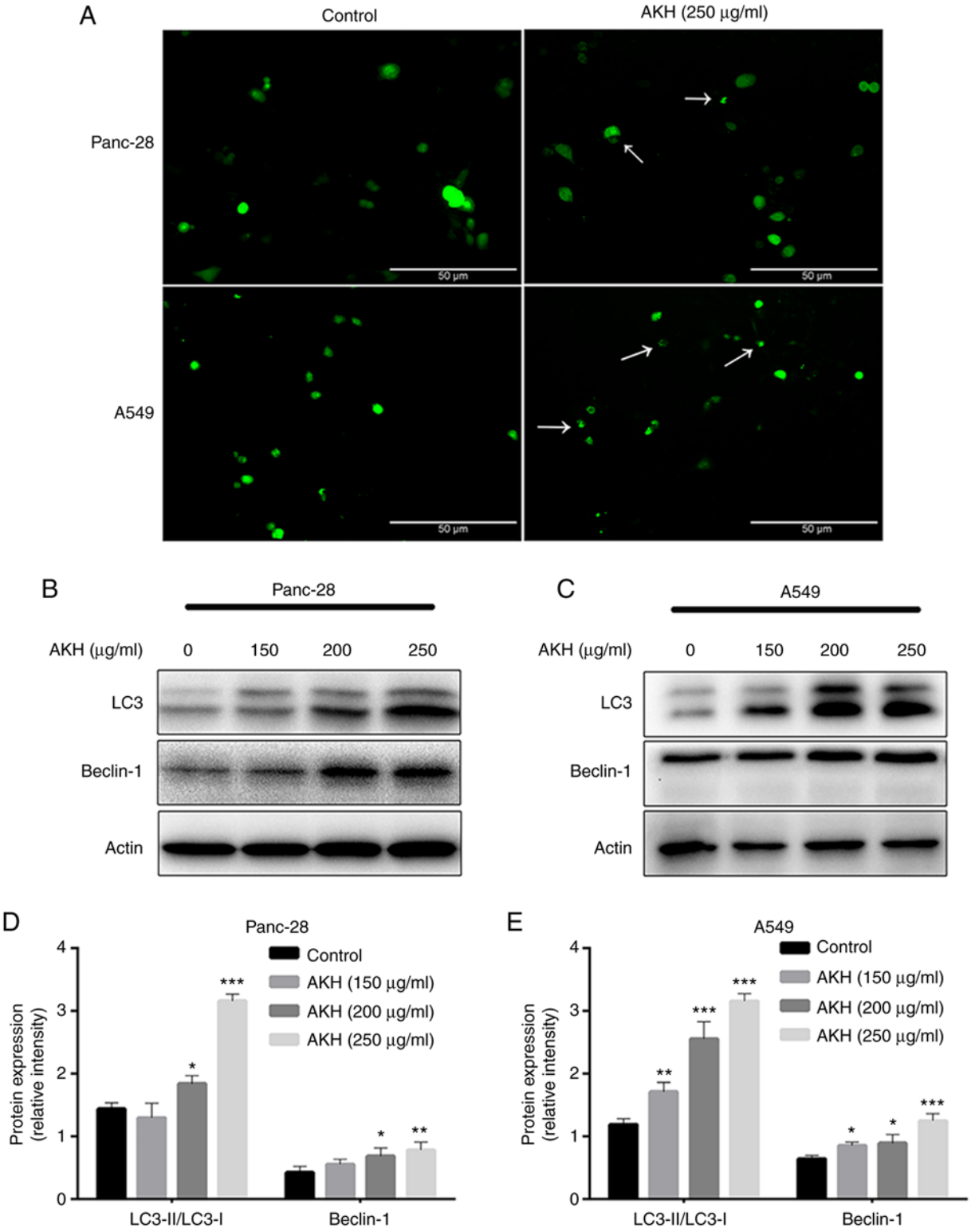

Figure 3. *Alpinia katsumadai Hayata* (AKH) induces autophagy in Panc-28 and A549 cells. (A) The formation of GFP-LC3 puncta in Panc-28 and A549 was examined under a fluorescence microscope (magnification, x200; white arrows indicate autophagic cells). The cells were treated with the vehicle control or AKH (250 μg/ml) for 48 h. (B) The bands of LC3, Beclin-1 and actin in Panc-28 cells were examined using western blot analysis. (C) The bands of LC3, Beclin-1 and actin in A549 cells by western blot analysis. Actin was used as a loading control. (D) Relative protein expression of LC-3 and Beclin-1 in Panc-28 cells. (E) Relative protein expression of LC-3 and Beclin-1 in A549 cells. (B-E) The cells were treated with the vehicle control or AKH at 150, 200 and 250 μg/ml for 48 h. Results are representative of three independent experiments (n=3) run in triplicate and are expressed as the mean ± SD. *P<0.05, **P<0.01 and ***P<0.001 vs. vehicle control (determined using one-way ANOVA).

antitumor activity of AKH (100 and 400 mg/kg) compared to that of normal saline (negative vehicle control) and cisplatin (5 mg/kg, positive control) in nude mice bearing A549 tumor xenografts; the results are illustrated in Fig. 6. The data indicated the kinetics of tumor growth (Fig. 6A) and the images of tumors (Fig. 6B) at the end of experiment following

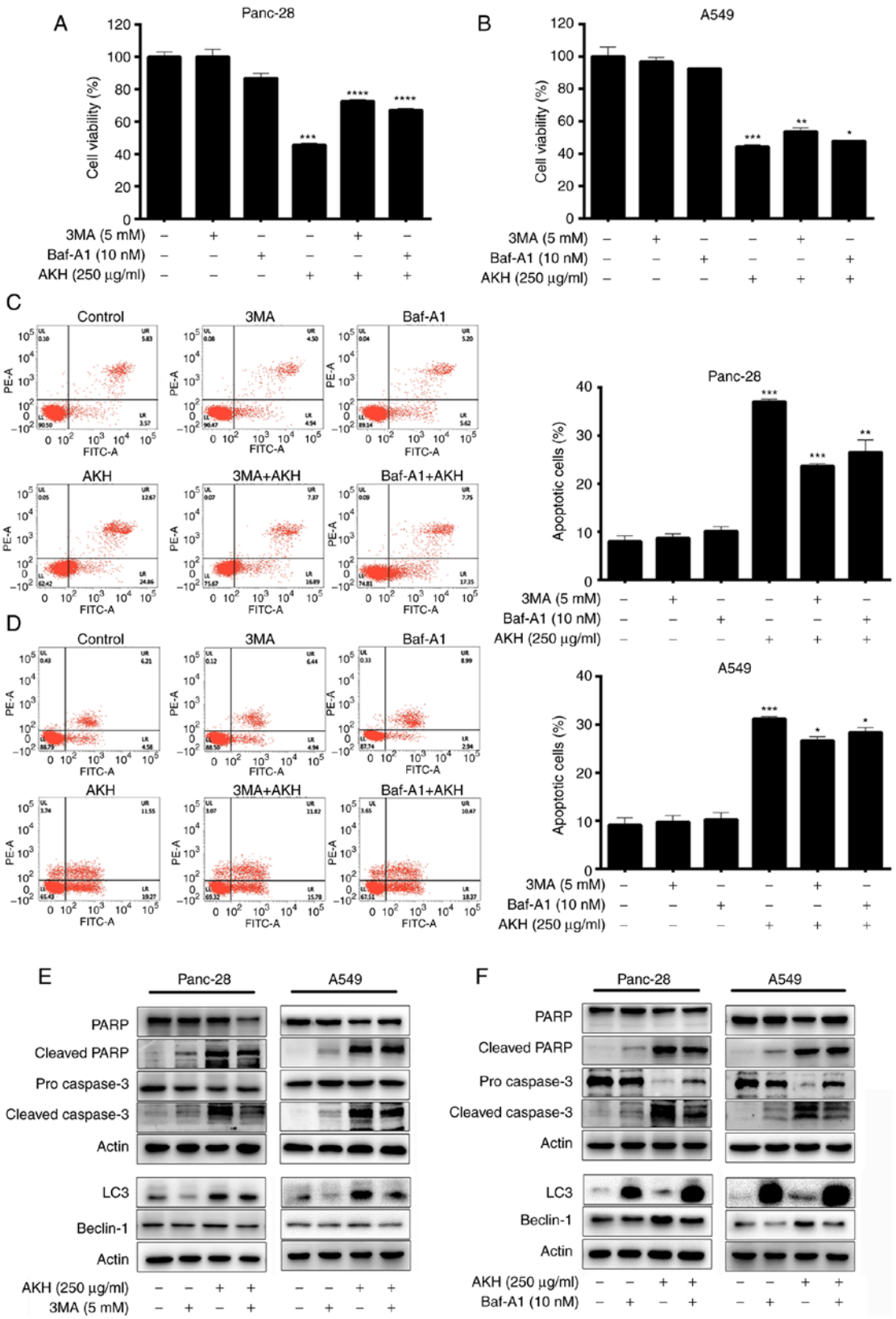

Figure 4. Effects of the autophagy inhibitors, 3MA and Baf-A1, on AKH-induced cell growth inhibition, apoptosis, and the expression of apoptosis- and autophagy-related proteins in Panc-28 and A549 cells. (A) The viability of the Panc-28 cells by CCK-8 assay. (B) The viability of the A549 cells by CCK-8 assay. (C) Flow cytometric analysis of Panc-28 cells. (D) Flow cytometric analysis of A549 cells. (E) The bands of apoptosis-related proteins PARP, cleaved-PARP, pro-caspase-3 and cleaved-caspase-3; autophagy-related proteins LC3, Beclin-1 and actin following treatment of 3MA and AKH alone or in combination in Panc-28 and A549 cells by western blot analysis. (F) The bands of apoptosis-related proteins PARP, cleaved-PARP, pro-caspase-3 and cleaved-caspase-3, autophagy-related proteins LC3, Beclin-1 and actin following treatment of Baf-A1 and AKH alone or in combination in Panc-28 and A549 cells by western blot analysis. Actin was used as a loading control. The cells were pre-treated with the vehicle control, 3MA (5 mM) or Baf-A1 (10 nM) for 24 h followed by the vehicle control or AKH (250 μg/ml) for 48 h. The data are representative of three independent experiments (n=3) run in triplicate and are expressed as the mean ± SD. *P<0.05, **P<0.01 and ***P<0.001 vs. vehicle control (determined using one-way ANOVA). AKH, *Alpinia katsumadai Hayata*; PARP, poly(ADP-ribose)polymerase; 3MA, 3-methyladenine; Baf-A1, baflomycin A1.

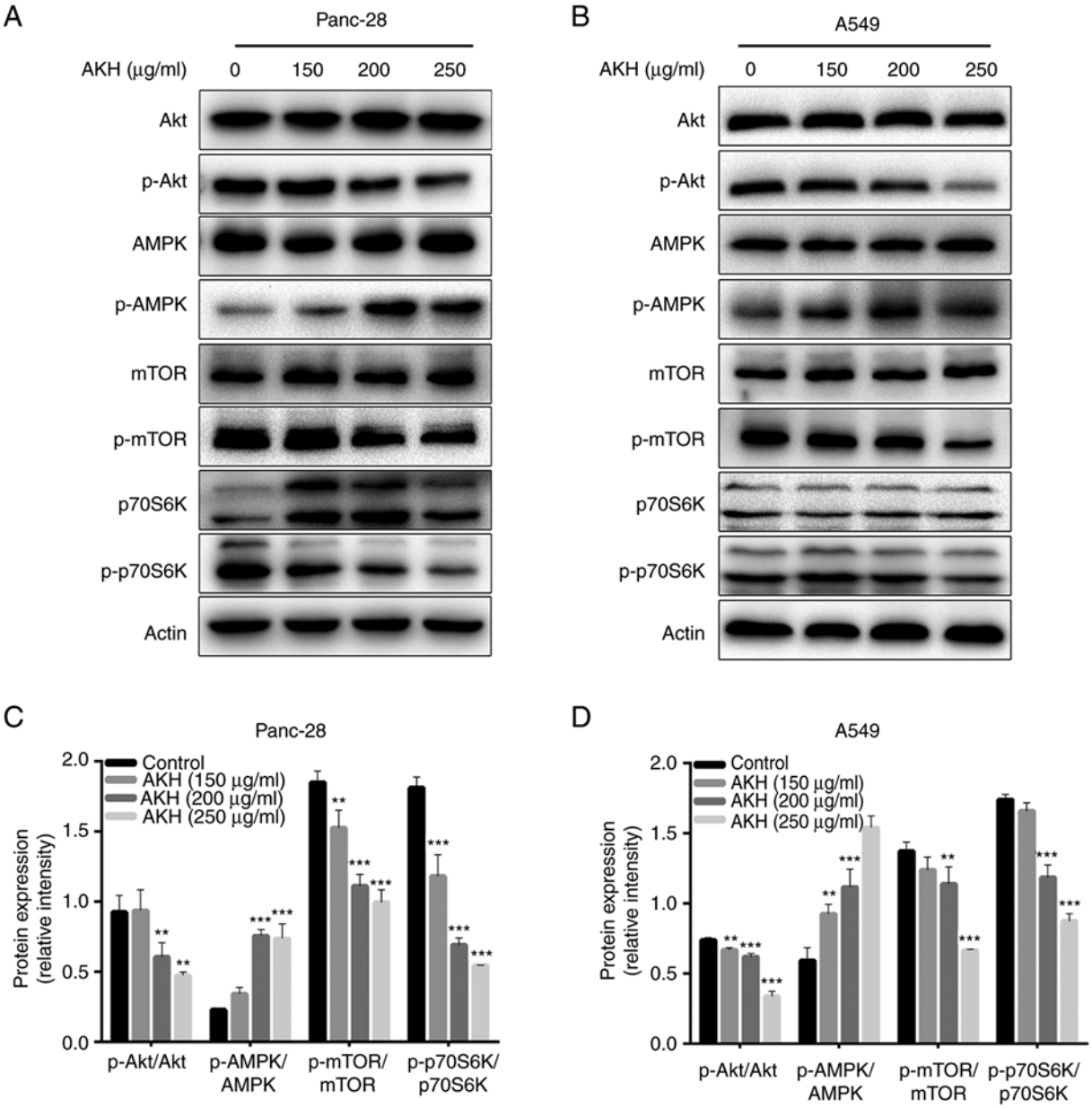

Figure 5. The effect of AKH on the expression of proteins related to the AMPK and Akt/mTOR/p70S6K singling pathways in Panc-28 and A549 cells by western blot analysis. (A) Bands of Akt, pAkt, AMPK, pAMPK, mTOR, pmTOR, 70S6K p70S6K and Actin in Panc-28 cells. (B) Bands of Akt, pAkt, AMPK, pAMPK, mTOR, pmTOR, 70S6K p70S6K and Actin in A549 cells. Actin was used as a loading control. (C) Relative protein expression of pAkt/Akt, pAMPK/AMPK, pmTOR/mTOR and p70S6K/70S6K in Panc-28 cells. (D) Relative protein expression of pAkt/Akt, pAMPK/AMPK, pmTOR/mTOR and p-p70S6K/p70S6K in A549 cells. The cells were treated with the vehicle control or AKH at 150, 200, and 250 μg/ml for 48 h. The data are representative of three independent experiments (n=3) run in triplicate and are expressed as the mean ± SD. **P<0.01 and ***P<0.001 vs. vehicle control (determined using one-way ANOVA). AKH, *Alpinia katsumadai Hayata*; AMPK, AMP-activated protein kinase.

the completion of treatment with normal saline, cisplatin or AKH in nude mice bearing A549 tumor xenografts. The results indicated that while normal saline had no significant antitumor effect, cisplatin and AKH significantly inhibited the growth of A549 tumor xenografts (P<0.01 or P<0.001). The mean tumor inhibitory rates were 50.40±8.23, 42.40±9.87 and 72.72±4.96% for cisplatin, 100 mg/kg AKH and 400 mg/kg AKH, respectively. Of note, the antitumor effects of AKH occurred in a dose-dependent manner and the antitumor efficacy of high-dose AKH (400 mg/kg) was significantly more prominent than that of cisplatin (P<0.01). Furthermore, no treatment-related death occurred, and the body weight loss of the mice was much less with AKH treatment (<10%) compared to that of cisplatin treatment (>15%; data not shown). These data indicated that AKH was effective against A549 tumor xenografts and safe to the hosts with better antitumor activity and less toxicity compared to that of cisplatin *in vivo*.

Analysis of the compositions of AKH by LCMS-IT-TOF. Finally, the present study determined the compositions of AKH using LCMS-IT-TOF assay with 0.5% formic acid in water and acetonitrile for separation. A total of nine components were detected from AKH using this assay (Fig. 7A). The nine compounds on their UV spectra were identified as pinocembrin,

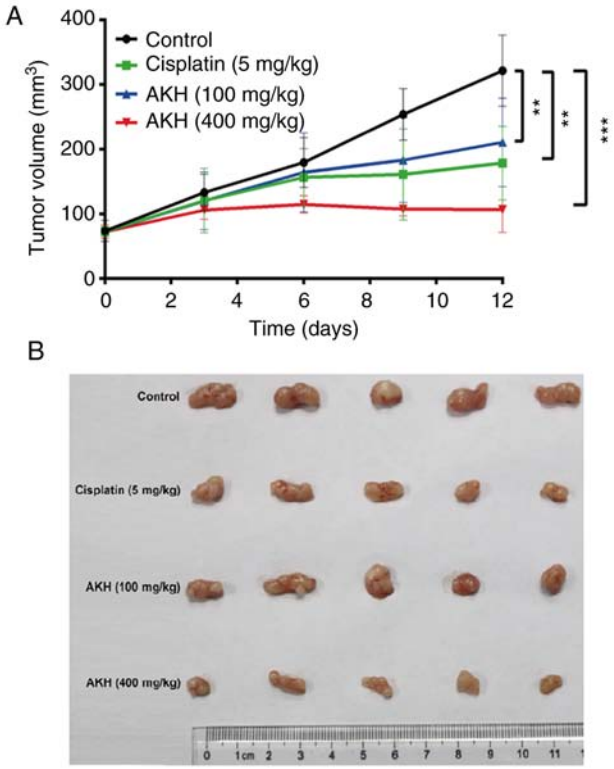

Figure 6. AKH inhibits the tumor growth of A549 xenografts in nude mice *in vivo*. (A) The kinetics of tumor growth. (B) Images of tumors at the end of experiment. The mice were administered normal saline (vehicle control), cisplatin (5 mg/kg/day, positive control) or AKH (100 and 400 mg/kg/day). AKH and normal saline were orally administered by gavage once a day for 12 days and cisplatin by intraperitoneal injection every 3 days for a total of five times (on days 0, 3, 6, 9 and 12). A total of 5 mice were used in each group. The data are expressed as the mean ± SD. **P<0.01 and ***P<0.001 vs. vehicle control (determined using one-way ANOVA). AKH, *Alpinia katsumadai Hayata*.

trans,trans-1,7-diphenyl-1,3-heptadien-5-ol,cardamomin, (-)-2-(1,2,3,4,4a,7-hexahydro-4a,8-dimethyl-1,7-dioxo-2-naphthyl)-propionic acid, (1E,4Z)-5-hydroxy-1-phenylhexa-1,4-dien-3-one, trans,trans-1,7-diphenyl-5-hydroxy-4,6-hepten-3-one, 1,7-diphenyl-4,6-heptadien-3-one, katsumadain B and (4E,6E)-5-hydroxy-1,7-diphenylhepta-4,6-dien-3-one, respectively. The chemical structures and characteristics of compounds identified from AKH are summarized in (Fig. 7B and Table II).

Discussion

Cancer is one of the most critical public health concerns and a leading cause of morbidity and mortality worldwide (2). It caused almost 10 million deaths worldwide in 2020 (35). Lung cancer is the second most diagnosed cancer with an estimated 2.2 million new cases and the leading cause of cancer death (1.8 million) globally in 2020 (35). Pancreatic cancer has a poor prognosis and a low survival rate, with 466,000 deaths reported 2020 worldwide (35). It has been indicated that only ~15% of patients with pancreatic cancer are diagnosed at the early stages upon disease progression (36). Therefore, the present study focused on the anticancer effects of AKH and associated molecular mechanisms in A549 lung cancer and Panc-28 pancreatic cancer cells.

Firstly, the present study investigated the anticancer effects of AKH in seven cancer cell lines, including Panc-28, A549, MDA-MB-468, Hela, A875, U87 and HCT-116, and compared these to those in normal human hepatic stellate LX-2 cells using CCK-8 assay. The results revealed that AKH displayed potent cytotoxicity against the tested cancer cells with IC_{50} values of 203-284 μg/ml; the Panc-28 and A549 cells were the most sensitive cells as regards the response to AHK treatment (Fig. 1A and Table I). Notably, AHK was much less cytotoxic against normal liver LX-2 cells with an IC_{50} of value of 395 μg/ml (Fig. 1A and Table I). These results indicated that AKH could selectively inhibit cancer cells. Subsequently, the time-dependent effects of AKH on the growth inhibition in Panc-28 and A549 cells were examined following treatment with AKH at 0 (control), 100, 150, 200, 250, 300 and 400 μg/ml for 24, 48 and 72 h, respectively. The results revealed that the inhibitory effects of AKH occurred in a concentration- and time-dependent manner; AKH was more effective at 48 and 72 h than at 24 h (P<0.001) in the Panc-28 and A549 cells (Fig. 1Ba and Bb).

Apoptosis and autophagy play a critical role in the fate of cancer and cancer therapy (19,31,37). Previous studies have demonstrated that apoptosis and autophagy are highly connected, and their association is very complex (28,35). Some active components from TCM have been proven to be effective against various types of cancer by inducing apoptosis and autophagy-related apoptosis (19,31,38-41). The present study found that AKH induced typical morphological features of apoptosis, such as chromatin condensation, nuclear shrinkage and apoptotic body formation in the Panc-28 and A549 cells by Hoechst 33342/PI staining assay (Fig. 2A and B). AKH also significantly increased the apoptotic rate in a concentration-dependent manner in the Panc-28 and A549 cells by quantitative analysis of flow cytometry with Annexin V-FITC/PI double staining assay (Fig. 2C-F). Furthermore, AKH significantly increased the expression of apoptosis-related proteins, such as cleaved PARP, caspase-8, cleaved caspase-3 and caspase-9 in a concentration-dependent manner in the Panc-28 and A549 cells, as demonstrated by western blot analysis (Fig. 2G and H). Moreover, treatment with AKH (150-250 μg/ml) for 48 h significantly induced autophagy, as evidenced by increased diffuse green spots, the formation and conversion of LC3-II and the increased expression of Beclin-1 in a concentration-dependent manner (Fig. 3).

It has been demonstrated that oridonin-induced apoptosis is attenuated by 3MA (an autophagy specific inhibitor) in human breast cancer cells, indicating that oridonin-induced autophagy participated in the upregulation of apoptosis (38). Another study also demonstrated that treatment with 3MA and Baf-A1 (another autophagy specific inhibitor) enhanced the salidroside-induced apoptosis of HT-29 colon cancer cells, indicating that salidroside-mediated autophagy may negatively regulate apoptosis to protect cancer cells from programmed cell death (40). In the present study, it was demonstrated that 3MA and Baf-A1 significantly decreased the effects of AKH on cell growth inhibition, apoptosis and autophagy induction, and the expression of apoptosis- and autophagy-related proteins, including cleaved PARP, pro- and cleaved caspase-3 and Beclin-1 in the Panc-28 and A549 cells (Fig. 4). Therefore, these results confirmed that

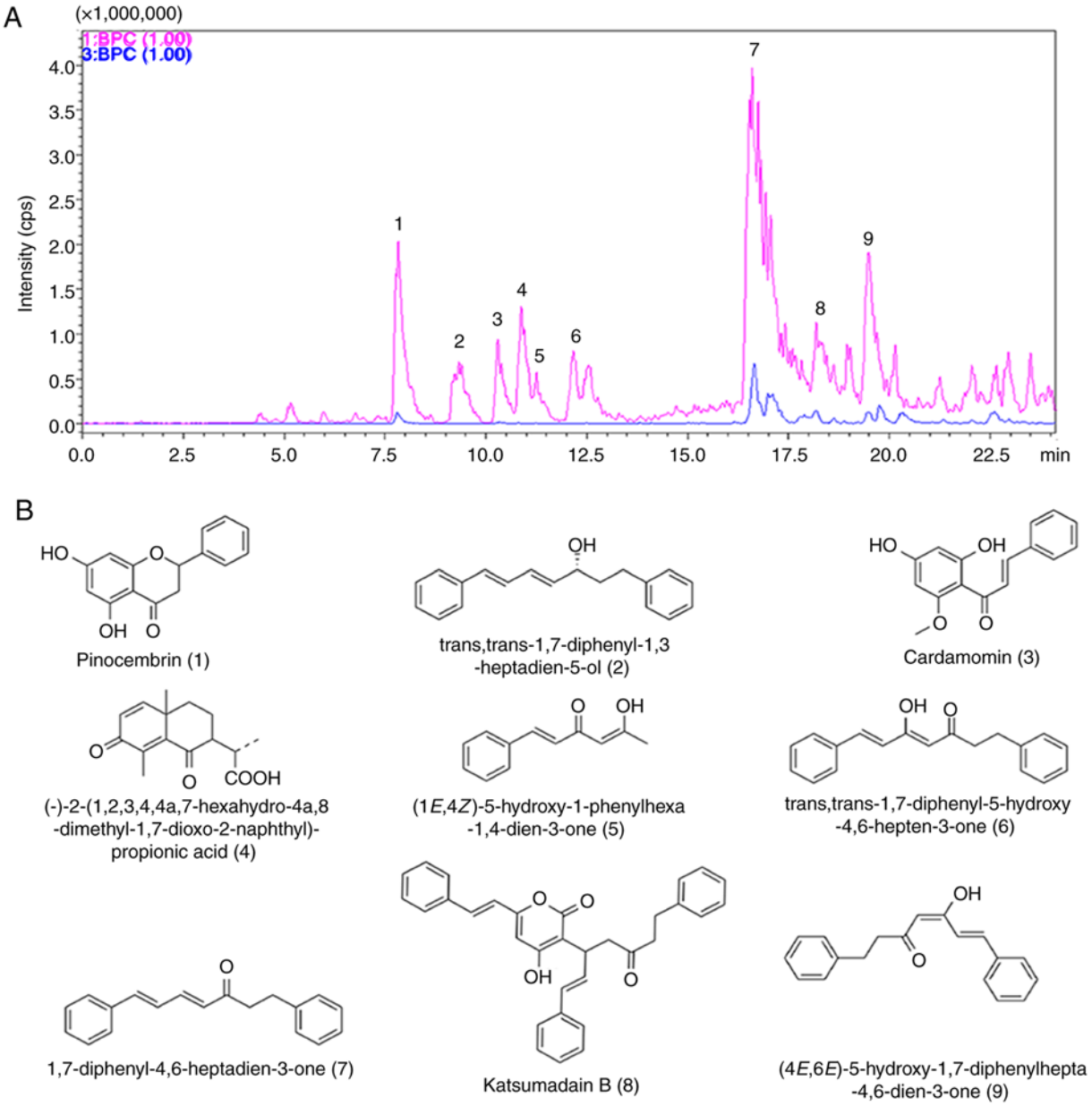

Figure 7. Analysis of the composition from AKH by LCMS-IT-TOF. (A) The BPC spectrum of AKH. (B) Chemical structures of AKH compounds detected by LCMS-IT-TOF. The nine compounds (1-9) are indicated in the figure and also listed in Table II. AKH, *Alpinia katsumadai Hayata*; LCMS-IT-TOF, liquid chromatography mass spectrometry-ion trap-time-of-flight mass spectrometry.

AKH induced autophagy-related apoptosis and the data are consistent with those of previous studies (38,40).

Akt/mTOR/p70S6K is one of the major pathways of autophagy and the activation of Akt/mTOR/p70S6K can inhibit autophagy (41). mTOR plays a central role by negatively controlling autophagy and phosphorylation of AMPK inhibits the mTOR signaling pathway, thereby activating autophagy (15,42). AMPK can also regulate apoptosis and autophagy by affecting the activation of p53, Bax, Bak and the caspase cascade (37). The present study found that AKH significantly increased the levels of p-AMPK and decreased those of p-Akt and its downstream target proteins, p-mTOR and p-70S6K in the Panc-28 and A549 cells (Fig. 5). Therefore, the AMPK and Akt/mTOR/p70S6K signaling pathways play key roles in the AKH-induced growth inhibition and apoptosis/autophagy induction in cancer cells.

To successfully develop an effective novel anticancer drug clinically, it must be validated using *in vivo* animal studies and clinical trials in order to confirm whether it is highly active against tumors with tolerated toxicity to the host. The establishment of transplanted human tumors in nude mice is an ideal approach to carry out studies on antitumor activity and subsequently, pharmacology *in vivo* (43). Therefore, the present study established the A549 xenograft model to investigate the antitumor effects of AKH *in vivo*. The result revealed that AKH was active against A549 human lung cancer tumor xenografts with tolerated toxicity to the host (Fig. 6). AKH displayed significant *in vivo* antitumor activity in a dose-dependent manner and high-dose AKH (400 mg/kg) exerted more prominent antitumor effects and less toxicity compared with cisplatin, with the tumor inhibition rates of 72.72% for AKH and 50.40% for cisplatin. According to the

Table II. Analysis of the characterized compounds from AKH.

Compound no.	Retention time (min)	Molecular weight (Da)	Molecular formula	Unsaturation	MS fragmentation (error in mDa)	Ultraviolet absorption (λ_{max}) nm	Structure or type of compound
1	7.78	256	$C_{15}H_{12}O_4$	10	Pos: 257.0889 [$(M+H)^+$, 8.1] Neg: 255.0680 [$(M-H)^-$, 1.7]	216, 289	Pinocembrin
2	9.33	264	$C_{19}H_{20}O$	10	Pos: 265.1605 [$(M+H)^+$, 1.8] MS/MS 247.1500 [$(M+H)^+$, 1.9]	250, 331	Trans,trans-1,7-diphenyl-1,3-heptadien-5-ol
3	10.28	270	$C_{16}H_{14}O_4$	10	Pos: 271.0995 [$(M+H)^+$,3.0] Neg:269.0787 [(M-H)-, -3.2]	215, 344	Cardamomin
4	10.92	262	$C_{15}H_{18}O_4$	7	Pos: 263.1350 [$(M+H)^+$, 7.2]	218, 250	(-)-2-(1,2,3,4,4a,7-Hexahydro-4a,8-dimethyl-1,7-dioxo-2-naphthyl)-propionic acid
5	11.26	188	$C_{12}H_{12}O_2$	7	Pos: 189.0877 [$(M+H)^+$, 3.3]	225, 340	(1E,4Z)-5-Hydroxy-1-phenylhexa-1,4-dien-3-one
6	12.17	278	$C_{19}H_{18}O_2$	11	Pos: 279.1347 [$(M+H)^+$, 2.0]	219, 331	Trans,trans-1,7-diphenyl-5-hydroxy-4,6-hepten-3-one
7	16.65	262	$C_{19}H_{18}O$	11	Pos: 263.1498 [$(M+H)^+$, 6.8]	231, 355	1,7-Diphenyl-4,6-heptadien-3-one
8	18.18	476	$C_{32}H_{28}O_4$	19	Pos: 477.2004 [$(M+H)^+$, -5.6] Neg:475.1913 [$(M-H)^-$, -0.2]	229, 325	Katsumadain B
9	19.51	278	$C_{19}H_{18}O_2$	11	Pos: 279.1346 [$(M+H)^+$, 2.0] Neg: 277.1174 [$(M-H)^-$, -6.0]	229, 361	(4E,6E)-5-Hydroxy-1,7-diphenylhepta-4,6-dien-3-one

Pos, detection in positive ion mode; Neg, detection in negative ion mode.

formula of human equivalent dose (HED) calculation as HED (mg/kg)=Animal does (mg/kg) x (animal Km/human Km) Eq, 400 mg/kg of AKH in mice is equal to 1,626 mg in an individual of 50 kg (44). AKH is a preparation of TCM and the used dosage of the ingredients of TCM is relatively high for the treatment of various diseases clinically. For example, the daily dose of Jinlida granule is ~27 g for diabetes mellitus treatment (45). Hua Shi Bai Du granule is used at a daily dose of 20 g in the treatment of coronavirus disease (46). Therefore, the preparations of TCM, including AKH can be applied to a dose of 20 g clinically. However, the clinical doses of AKH and/or its active components should be based on the results of preclinical pharmacodynamics, pharmacokinetics, efficacy and toxicology, as well as phase I clinical trials. Therefore, AKH has the potential to be further developed for the treatment of patients with lung cancer clinically. However, further studies on AKH and/or its active fractions for the antitumor efficacy and toxicity are warranted, with various animal models of human tumor xenografts *in vivo* and validation by clinical trials. In the *in vivo* experiments from the present study, AKH only significantly suppressed the growth of A549 lung cancer xenografts but did not shrink the original size of the tumors. In general, the combination of an anticancer agent extracted from TCM and a chemotherapeutic drug could enhance the antitumor efficacy and reduce the side-effects of chemotherapy. Therefore, the clinical application of AKH in cancer therapy is expected to be combined with chemotherapeutic, targeted therapeutic and/or immunotherapeutic agents.

Furthermore, the compositions of AKH were determined by LCMS-IT-TOF analysis and nine compounds were detected from AKH namely pinocembrin, trans,trans-1, 7-diphenyl-1,3-heptadien-5-ol, cardamomin, (-)-2-(1,2,3,4,4a, 7-haxahydro-4a,8-dimethyl-1,7-dioxo-2-naphthyl)-propionic acid, (1E,4Z)-5-hydroxy-1-phenylhexa-1,4-dien-3-one, trans,trans-1,7-diphenyl-5-hydroxy-4,6-hepten-3-one, 1, 7-diphenyl-4,6-heptadien-3-one, katsumadain B and (4E,6E)-5-hydroxy-1,7-diphenylhepta-4,6-dien-3-on-e, respectively (Fig. 7 and Table II). These findings indicated that AKH mainly contains chalcones and diarylheptanoids. Pinocembrin exerts anti-inflammatory, anti-bacterial and anticancer effects (47,48). Studies have shown that pinocembrin inhibits the proliferation, migration and invasion of breast cancer cells at non-cytotoxic concentrations by inhibiting the STAT3 signaling pathway (48). Cardamonin is the main flavonoid derived from AKH and exerts anti-proliferative effects against various cancer cells (49). Another study demonstrated that the anticancer effects of cardamonin were associated with autophagy in HCT-116 cells (23). In a previous study by the authors, it was also shown that cardamonin induced the apoptosis of glioblastoma stem cells by suppressing the STAT3 signaling pathway (30). However, the study of katsumadain B is only limited to its anti-emetic effect (50). Therefore, pinocembrin and cardamonin may play key roles in the anticancer activity of AKH. IT has been indicated that alpinetin is one of the main constituents of AKH and that it is involved in its antitumor effect (51,52). However, the present study could not detect alpinetin using LCMS-IT-TOF, which is inconsistent with the aforementioned studies.

Finally, the model of the possible underlying molecular mechanisms associated with the effects of AKH on the apoptosis and autophagy in human cancer cells was proposed in (Fig. 8). AKH induces caspase-mediated apoptosis by increasing the expression of caspase-8, caspase-9, cleaved caspase-3 and cleaved PARP. Moreover, AKH not only promotes apoptosis, but also activates autophagy. AKH inhibits the activation of the Akt/mTOR/p70S6K signaling pathway by increasing the levels of p-AMPK, and decreasing those of p-Akt, p-mTOR and p-70S6K, thereby activating autophagy.

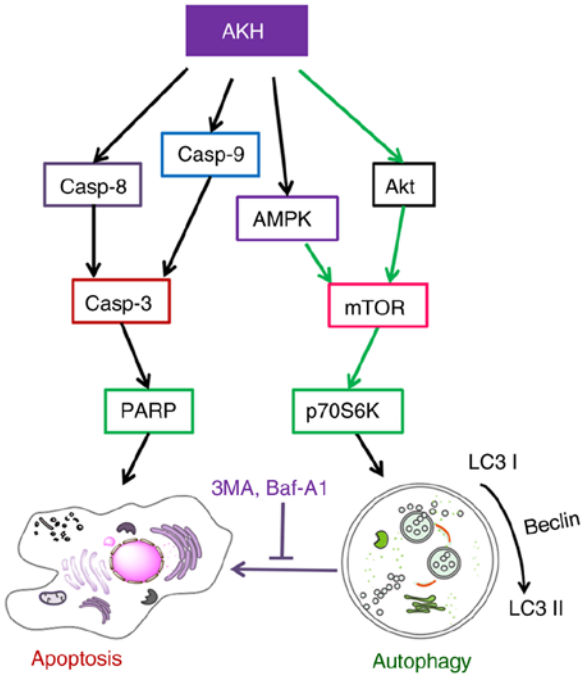

Figure 8. A proposed schematic model of the underlying molecular mechanism associated with the effects of AKH on apoptosis and autophagy in human cancer cells. The black lines indicate activation and the green lines indicate inhibition. AKH, *Alpinia katsumadai Hayata;* AMPK, AMP-activated protein kinase; PARP, poly(ADP-ribose)polymerase; 3MA, 3-methyladenine; Baf-A1, baflomycin A1; Casp, caspase.

In conclusion, the present study demonstrated that AKH selectively inhibited the proliferation of various cancer cells, whereas it exerted much less potent inhibitory effects on normal liver cells. AKH significantly induced cellular apoptosis and autophagy by regulating the AMPK and Akt/mTOR/p70S6K signaling pathways in Panc-28 pancreatic cancer and A549 lung cancer cells *in vitro*. Furthermore, AKH significantly inhibited tumor growth with better antitumor efficacy and less toxicity compared to that of cisplatin (a commonly used anticancer drug in clinic) in nude mice bearing A549 tumor xenografts *in vivo*. In addition, nine components were identified from AKH by LCMS-IT-TOF assay. Therefore, the findings presented herein may provide the scientific rationale for the understanding of the anticancer effects of AKH and associated mechanisms of action. AKH and its active fractions may have the potential to be developed as novel anticancer agents clinically.

Acknowledgements

Not applicable.

Funding

The present study was supported by the International Collaborative Project of the MOST of China (grant no. 2017YFE0195000), the Taishan Talents project of Shandong province and the Natural Science Foundation in Shandong Province of China (grant nos. ZR2020MH420, ZR2020MH421 and ZR2020QH360), and the Distinguished Professor Research Startup Funding from Southwest Medical University (grant no. 2015-RCYJ0002).

Availability of data and materials

The datasets used and/or analyzed during the current study are available from the corresponding author on reasonable request.

Authors' contributions

SC and XL provided the funding and designed the study, supervised the experiments, and analyzed the data. WA, YZ, HL and YZ performed the experiments. HZ, GZ, YL and ML analyzed the data and prepared the figures. WA, YZ and SC wrote the manuscript. WA and HL confirm the authenticity of all the raw data. All authors have read and approved the final version of the manuscript.

Ethics approval and consent to participate

All animal experiments were approved (permit no. 201802-112) by the Institutional Animal Care and Use Committee of Southwest Medical University (Luzhou, China) and strictly followed the guidelines for the investigation of experimental pain in conscious animals for improving animal welfare to minimize animal suffering (29).

Patient consent for publication

Not applicable.

Competing interests

The authors declare that they have no competing interests.

References

1. Adams C, Grey N, Magrath I, Miller A and Torode J: The world cancer declaration: Is the world catching up? Lancet Oncol 11: 1018-1020, 2010.
2. Siegel RL, Miller KD and Jemal A: Cancer statistics, 2020. CA Cancer J Clin 70: 7-30, 2020.
3. Qiu X and Jia J: Research advances on TCM anti-tumor effects and the molecular mechanisms. J Cancer Res Ther 10 (Suppl 1): S8-S13, 2014.
4. Li Z, Feiyue Z and Gaofeng L: Traditional Chinese medicine and lung cancer-from theory to practice. Biomed Pharmacother 137: 111381, 2021.
5. Kerr JF, Wyllie AH and Currie AR: Apoptosis: A basic biological phenomenon with wide-ranging implications in tissue kinetics. Br J Cancer 26: 239-257, 1972.
6. Lim HS, Seo CS, Ha H, Lee H, Lee JK, Lee MY and Shin H: Effect of *Alpinia katsumadai Hayata* on house dust mite-induced atopic dermatitis in NC/Nga mice. Evid Based Complement Alternat Med 2012: 705167, 2012.
7. Wu H, Che X, Zheng Q, Wu A, Pan K, Shao A, Wu Q, Zhang J and Hong Y: Caspases: A molecular switch node in the crosstalk between autophagy and apoptosis. Int J Biol Sci 10: 1072-1083, 2014.
8. Mizushima N: Autophagy: Process and function. Genes Dev 21: 2861-2873, 2007.
9. Yang Z and Klionsky DJ: An overview of the molecular mechanism of autophagy. Curr Top Microbials Immunol 335: 1-32, 2009.
10. Panda PK, Mukhopadhyay S, Das DN, Sinha N, Naik PP and Bhutia SK: Mechanism of autophagic regulation in carcinogenesis and cancer therapeutics. Semin Cell Dev Biol 39: 43-55, 2015.
11. White E: Deconvoluting the context-dependent role for autophagy in cancer. Nat Rev Cancer 12: 401-410, 2012.
12. Ávalos Y, Canales J, Bravo-Sagua R, Criollo A, Lavandero S and Quest AF: Tumor suppression and promotion by autophagy. Biomed Res Int 2014: 603980, 2014.
13. Meijer AJ and Codogno P: Regulation and role of autophagy in mammalian cells. Int J Biochem Cell Biol 36: 2445-2462, 2004.
14. Codogno P and Meijer AJ: Autophagy and signaling: Their role in cell survival and cell death. Cell Death Differ 12 (Suppl 2): S1509-S1518, 2005.
15. Matsui Y, Takagi H, Qu X, Abdellatif M, Sakoda H, Asano T, Levine B and Sadoshima J: Distinct roles of autophagy in the heart during ischemia and reperfusion: Roles of AMP-activated protein kinase and beclin 1 in mediating autophagy. Circ Res 100: 914-922, 2007.
16. Scott RC, Juhász G and Neufeld TP: Direct induction of autophagy by Atg1 inhibits cell growth and induces apoptotic cell death. Curr Biol 17: 1-11, 2007.
17. Bousman CA, Chana G, Glatt SJ, Chandler SD, Lucero GR, Tatro E, May T, Lohr JB, Kremen WS, Tsuang MT and Everall IP: Preliminary evidence of ubiquitin proteasome system dysregulation in schizophrenia and bipolar disorder: Convergent pathway analysis findings from two independent samples. Am J Med Genet B Neuropsychiatr Genet 153B: 494-502, 2010.
18. Wang CY, Bai XY and Wang CH: Traditional Chinese medicine: A treasured natural resource of anticancer drug research and development. Am J Chin Med 42: 543-559, 2014.
19. An W, Lai H, Zhang Y, Liu M, Lin X and Cao S: Apoptotic pathway as the therapeutic target for anticancer traditional Chinese medicines. Front Pharmacol 10: 758, 2019.
20. Chinese Pharmacopoeia Commission: Chinese Pharmacopoeia, 2020. Beijing, China: Chinese Medicine Science and Technology Press, Part 1, pp249, 2020.
21. Lee MY, Lee NH, Seo CS, Lee JA, Jung D, Kim JH and Shin HK: *Alpinia katsumadai* seed extract attenuate oxidative stress and asthmatic activity in a mouse model of allergic asthma. Food Chem Toxicol 48: 1746-1752, 2010.
22. Du J, Tang B, Wang J, Sui H, Jin X, Wang L and Wang Z: Antiproliferative effect of alpinetin in BxPC-3 pancreatic cancer cells. Int J Mol Med 29: 607-612, 2012.
23. Kim YJ, Kang KS, Choi KC and Ko H: Cardamonin induces autophagy and an antiproliferative effect through JNK activation in human colorectal carcinoma HCT116 cells. Bioorg Med Chem Lett 25: 2559-2564, 2015.
24. Wang XB, Yang CS, Luo JG, Zhang C, Luo J, Yang MH and Kong LY: Experimental and theoretical calculation studies on the structure elucidation and absolute configuration of calyxins from *Alpinia katsumadai*. Fitoterapia 119: 121-129, 2017.
25. Liu M, Zhao G, Zhang D, An W, Lai H, Li X, Cao S and Lin X: Active fraction of clove induces apoptosis via PI3K/Akt/mTOR-mediated autophagy in human colorectal cancer HCT-116 cells. Int J Oncol 53: 1363-1373, 2018.
26. Cao S, McGuire JJ and Rustum YM: Antitumor activity of ZD1694 (tomudex) against human head and neck cancer in nude mouse models: Role of dosing schedule and plasma thymidine. Clin Cancer Res 5: 1925-1934, 1999.
27. Cao S, Durrani FA, Tóth K and Rustum YM: Se-methylselenocysteine offers selective protection against toxicity and potentiates the antitumour activity of anticancer drugs in preclinical animal models. Br J Cancer 110: 1733-1743, 2014.
28. Kanzawa T, Zhang L, Xiao L, Germano IM, Kondo Y and Kondo S: Arsenic trioxide induces autophagic cell death in malignant glioma cells by upregulation of mitochondrial cell death protein BNIP3. Oncogene 24: 980-991, 2005.
29. Zimmermann M: Ethical guidelines for investigations of experimental pain in conscious animals. Pain 16: 109-110, 1983.

30. Wu N, Liu J, Zhao X, Yan Z, Jiang B, Wang L, Cao S, Shi D and Lin X: Cardamonin induces apoptosis by suppressing STAT3 signaling pathway in glioblastoma stem cells. Tumour Biol 36: 9667-9676, 2015.
31. Han C, Xing G, Zhang M, Zhong M, Han Z, He C and Liu X: Wogonoside inhibits cell growth and induces mitochondrial-mediated autophagy-related apoptosis in human colon cancer cells through the PI3K/AKT/mTOR/p70S6K signaling pathway. Oncol Lett 15: 4463-4470, 2018.
32. Shinojima N, Yokoyama T, Kondo Y and Kondo S: Roles of the Akt/mTOR/p70S6K and ERK1/2 signaling pathways in curcumin-induced autophagy. Autophagy 3: 635-637, 2007.
33. Dasgupta B and Chhipa RR: Evolving lessons on the complex role of AMPK in normal physiology and cancer. Trends Pharmacol Sci 37: 192-206, 2016.
34. Moore J, Megaly M, MacNeil AJ, Klentrou P and Tsiani E: Rosemary extract reduces Akt/mTOR/p70S6K activation and inhibits proliferation and survival of A549 human lung cancer cells. Biomed Pharmacother 83: 725-732, 2016.
35. Sung H, Ferlay J, Siegel RL, Laversanne M, Soerjomataram I, Jemal A and Bray F: Global cancer statistics 2020: GLOBOCAN estimates of incidence and mortality worldwide for 36 cancers in 185 countries. CA Cancer J Clin 71: 209-249, 2021.
36. Moutinho-Ribeiro P, Macedo G and Melo SA: Pancreatic cancer diagnosis and management: Has the time come to prick the bubble? Front Endocrinol (Lausanne) 9: 779, 2019.
37. Chaabane W, User SD, El-Gazzah M, Jaksik R, Sajjadi E, Rzeszowska-Wolny J and Los MJ: Autophagy, apoptosis, mitoptosis and necrosis: Interdependence between those pathways and effects on cancer. Arch Immunol Ther Exp (Warsz) 61: 43-58, 2013.
38. Li Y, Wang Y, Wang S, Gao Y, Zhang X and Lu C: Oridonin phosphate-induced autophagy effectively enhances cell apoptosis of human breast cancer cells. Med Oncol 32: 365, 2015.
39. Zhou ZW, Li XX, He ZX, Pan ST, Yang Y, Zhang X, Chow K, Yang T, Qiu JX, Zhou Q, *et al*: Induction of apoptosis and autophagy via sirtuin1- and PI3K/Akt/mTOR-mediated pathways by plumbagin in human prostate cancer cells. Drug Des Devel Ther 9: 1511-1554, 2015.
40. Fan XJ, Wang Y, Wang L and Zhu M: Salidroside induces apoptosis and autophagy in human colorectal cancer cells through inhibition of PI3K/Akt/mTOR pathway. Oncol Rep 36: 3559-3567, 2016.
41. Zhang HW, Hu JJ, Fu RQ, Liu X, Zhang YH, Li J, Liu L, Li YN, Deng Q, Luo QS, *et al*: Flavonoids inhibit cell proliferation and induce apoptosis and autophagy through downregulation of PI3Kγ mediated PI3K/AKT/mTOR/p70S6K/ULK signaling pathway in human breast cancer cells. Sci Rep 8: 11255, 2018.
42. Inoki K, Kim J and Guan KL: AMPK and mTOR in cellular energy homeostasis and drug targets. Annu Rev Pharmacol Toxicol 52: 381-400, 2012.
43. Wu CF, Wu CY, Chiou RY, Yang WC, Lin CF, Wang CM, Hou PH, Lin TC, Kuo CY and Chang GR: The anti-cancer effects of a zotarolimus and 5-fluorouracil combination treatment on A549 cell-derived tumors in Balb/c nude mice. Int J Mol Sci 22: 4562, 2021.
44. Nair AB and Jacob S: A simple practice guide for dose conversion between animals and human. J Basic Clin Pharm 7: 27-31, 2016.
45. Shi YL, Liu WJ, Zhang XF, Su WJ, Chen NN, Lu SH, Wang LY, Shi XL, Li ZB and Yang SY: Effect of Chinese herbal medicine Jinlida granule in treatment of patients with impaired glucose tolerance. Chin Med J (Engl) 129: 2281-2286, 2016.
46. Liu J, Yang W, Liu Y, Lu C, Ruan L, Zhao C, Huo R, Shen X, Miao Q, Lv W, *et al*: Combination of Hua Shi Bai Du granule (Q-14) and standard care in the treatment of patients with coronavirus disease 2019 (COVID-19): A single-center, open-label, randomized controlled trial. Phytomedicine 91: 153671, 2021.
47. Rasul A, Millimouno FM, Ali Eltayb W, Ali M, Li J and Li X: Pinocembrin: A novel natural compound with versatile pharmacological and biological activities. Biomed Res Int 2013: 379850, 2013.
48. Zhu X, Li R, Wang C, Zhou S, Fan Y, Ma S, Gao D, Gai N and Yang J: Pinocembrin inhibits the proliferation and metastasis of breast cancer via suppression of the PI3K/AKT signaling pathway. Front Oncol 11: 661184, 2021.
49. Gonçalves LM, Valente IM, Rodrigues JA: An overview on cardamonin. J Med Food 17: 633-640, 2014.
50. Yang Y, Kinoshita K, Koyama K, Takahashi K, Tai T, Nunoura Y and Watanabe K: Two novel anti-emetic principles of *Alpinia katsumadai*. J Nat Prod 62: 1672-1674, 1999.
51. Huo M, Chen N, Chi G, Yuan X, Guan S, Li H, Zhong W, Guo W, Soromou LW, Gao R, *et al*: Traditional medicine alpinetin inhibits the inflammatory response in Raw 264.7 cells and mouse models. Int Immunopharmacol 12: 241-248, 2012.
52. Zhao X, Guo X, Shen J and Hua D: Alpinetin inhibits proliferation and migration of ovarian cancer cells via suppression of STAT3 signaling. Mol Med Rep 18: 4030-4036, 2018.